

High-Energy Gamma-Ray Observations of Two Young, Energetic Radio Pulsars

V. M. Kaspi¹ and J. R. Lackey²

Department of Physics and Center for Space Research, Massachusetts Institute of Technology, 70 Vassar St., Cambridge, MA 02139

J. Mattox³

Astronomy Department, Boston University, 725 Commonwealth Ave., Boston, MA 02215

R. N. Manchester⁴

Australia Telescope National Facility, Epping, NSW, 2121 Australia

M. Bailes⁵

Astrophysics and Supercomputing, Swinburne University of Technology, Mail 31, PO Box 218, Hawthorn, Victoria, 3122 Australia

R. Pace⁶

Physics Department, University of Adelaide, Adelaide, SA, Australia

ABSTRACT

We present results of *Compton Gamma-Ray Observatory*/EGRET observations of the unidentified high-energy γ -ray sources 2EG J1049–5847 (GEV J1047–5840, 3EG J1048–5840) and 2EG J1103–6106 (3EG J1102–6103). These sources are spatially coincident with the young, energetic radio pulsars PSRs B1046–58 and J1105–6107, respectively. We find evidence for an association between PSR B1046–58 and 2EG J1049–5847. The γ -ray pulse profile, obtained by folding time-tagged photons having energies above 400 MeV using contemporaneous radio ephemerides, has probability of arising by chance of 1.2×10^{-4} according to the binning-independent H-test. A spatial analysis of the on-pulse

¹Alfred P. Sloan Research Fellow; vicky@space.mit.edu

²jes@space.mit.edu

³mattox@bu.edu

⁴rmanches@atnf.csiro.au

⁵mbailes@swin.edu.au

photons reveals a point source of equivalent significance 10.2σ . Off-pulse, the significance drops to 5.8σ . Archival *ASCA* data show that the only hard X-ray point source in the 95% confidence error box of the γ -ray source is spatially coincident with the pulsar within the $1'$ uncertainty (Pivovarov, Kaspi, & Gotthelf 1999). The double peaked γ -ray pulse morphology and leading radio pulse are similar to those seen for other γ -ray pulsars and are well-explained in models in which the γ -ray emission is produced in charge-depleted gaps in the outer magnetosphere. The inferred pulsed γ -ray flux above 400 MeV, $(2.5 \pm 0.6) \times 10^{-10}$ erg cm $^{-2}$ s $^{-1}$, represents 0.011 ± 0.003 of the pulsar's spin-down luminosity, for a distance of 3 kpc and 1 sr beaming. For PSR J1105–6107, light curves obtained by folding EGRET photons using contemporaneous radio ephemerides show no significant features. We conclude that this pulsar converts less than 0.014 of its spin-down luminosity into $E > 100$ MeV γ -rays beaming in our direction (99% confidence), assuming a distance of 7 kpc, 1 sr beaming and a duty cycle of 0.5.

Subject headings: gamma rays: observations — pulsars: general — pulsars: individual: PSR B1046–58, PSR J1105–6107

1. Introduction

An outstanding unknown in γ -ray astronomy is the nature of a population of high-energy γ -ray sources at low Galactic latitude which were first identified using the COS-B satellite (Swanenburg et al. 1981). More recently, these sources were studied in greater detail by the Energetic Gamma Ray Experiment Telescope (EGRET) aboard the *Compton Gamma-Ray Observatory* (Kanbach et al. 1996). In contrast to the high-energy γ -ray sources at high latitudes, which are typically associated with active galaxies, several dozen apparent point sources of high-energy γ -rays at latitudes $|b| \lesssim 10^\circ$ have as yet not been identified with astronomical objects. However, a handful of low-latitude sources has been identified with young, energetic radio pulsars (see Thompson 1996 for a review). This suggests that many of the unidentified sources are also young pulsars. This hypothesis has been considered in various studies, many of which suggest that the majority, if not all, of the unidentified sources are pulsars (Yadigaroglu & Romani 1995, Kaaret & Cottam 1996, Yadigaroglu & Romani 1997, Cheng & Zhang 1998). Sturmer & Dermer (1995) suggested that many of the sources are not pulsars but rather are a result of cosmic ray interactions with gas in supernova remnants. With the EGRET spatial resolution generally limited to tens of arcminutes, identification of discrete high-energy γ -ray sources is difficult using spatial coincidence alone, explaining why this problem has remained open so long.

Rotation-powered pulsars permit a straightforward determination of the nature of a γ -ray source using the signature pulsed emission. Indeed the Crab and Vela pulsars are long-known to be strong sources of pulsed γ -rays. EGRET has provided unambiguous and/or strong evidence for pulsations from five other rotation-powered pulsars (see Table 1). Five of the six pulsars having the highest values of the parameter \dot{E}/d^2 , where the spin-down luminosity $\dot{E} \equiv 4\pi^2 I \dot{P}/P^3$ (P is the pulse period and \dot{P} its rate of increase) and d is the distance to the source, are established sources of high-energy γ -ray pulsations. Finding rotation-powered pulsars at γ -ray energies is important because those detected thus far have their maximum luminosities in this energy range. Thus γ -rays may hold the key to the poorly understood pulsar energy budget and emission mechanism, in which mechanical energy of rotation is efficiently converted into non-thermal high-energy radiation. The origin of the γ -rays – whether at the neutron star polar cap (e.g. Daugherty & Harding 1996) or in the outer magnetosphere (e.g. Romani & Yadigaroglu 1995) – is still debated. In this paper we examine high-energy γ -ray data from the direction of two young, energetic pulsars which are good candidates for observable γ -ray pulsations.

PSR B1046–58 is a 124 ms radio pulsar having characteristic age 20 kyr and spin-down luminosity $\dot{E} = 2.0 \times 10^{36}$ erg s⁻¹. It was discovered in a survey of the Galactic plane for radio pulsars (Johnston et al. 1992), and has an unremarkable radio average pulse profile, characterized by a single narrow peak having width ~ 8 ms at 1.4 GHz (Figure 1). Its pulsed radio emission is highly linearly polarized and shows a slow position angle variation across the pulse, suggestive of conal emission (Qiao et al. 1995). The dispersion measure of 129.01 ± 0.01 pc cm⁻³ toward this pulsar implies a distance of 2.98 ± 0.35 kpc (Taylor & Cordes 1993). In the rank-ordered \dot{E}/d^2 list, PSR B1046–58 falls ninth, with six of the eight above it known γ -ray pulsars, five of those six being high-energy γ -ray sources (see Table 1). The pulsar’s position lies near the 95% confidence contour for the Second EGRET catalog source 2EG J1049–5847 (Thompson et al. 1995). Thompson et al. (1994) reported a pulsed flux 99.9% confidence upper limit for energies above 100 MeV of 4.5×10^{-7} photons cm⁻² s⁻¹ for a 50% duty cycle pulse. They noted, however, a “hint” of a pulsation for PSR B1046–58 above 1 GeV, having probability of chance occurrence of 14%. As reported in a companion paper, Pivovarov, Kaspi & Gotthelf (1999) have detected X-rays from the direction of the pulsar; that emission is not pulsed and is probably due to a synchrotron nebula.

PSR J1105–6107 is a 63 ms pulsar having characteristic age 63 kyr and $\dot{E} = 2.5 \times 10^{36}$ erg s⁻¹ (Kaspi et al. 1997). It exhibits a narrow double peaked radio pulse profile having width 3.4 ms at 1.6 GHz. Its radio emission is highly linearly polarized, showing a slow positional angle variation suggestive of conal emission (Crawford et al. 1999). The pulsar’s dispersion measure of 270.55 ± 0.14 pc cm⁻³ implies a distance of 7.1 ± 0.9 kpc (Taylor & Cordes 1993). Ranking by \dot{E}/d^2 , it is 23rd, well above the known γ -ray pulsar PSR B1055–52

(whose distance may well be overestimated; see Thompson et al. 1999 and references therein) though well below several sources which have not been detected by EGRET (Thompson et al. 1994). PSR J1105–6107 is spatially coincident with the unidentified EGRET source 2EG J1103–6106 (Thompson et al. 1995, Kaspi et al. 1997). This γ -ray source has pulsar-like properties: it has a hard spectrum and is not time variable. However the Second EGRET catalog noted marginal evidence for the source being extended. PSR J1105–6107 has been detected as an unpulsed X-ray source (Gotthelf & Kaspi 1998, Steinberger, Kaspi, & Gotthelf 1999); this emission is best explained as being due to nebular synchrotron emission powered by the pulsar wind.

Given the importance of identifying γ -ray pulsations in radio pulsars as well as establishing the nature of the unidentified EGRET sources, additional EGRET exposure of the Eta Carina region was obtained. We report here on an analysis of EGRET data for PSR B1046–58 obtained between 1991 May and 1997 October, and for PSR J1105–6107 between 1993 July and 1997 October. In §2 we summarize the EGRET observations used in our analysis. In §3 we report our findings, showing evidence for γ -ray pulsations from PSR B1046–58, but none from PSR J1105–6107. We discuss our results and their implications in §4.

2. Observations and Analysis

The Energetic Gamma Ray Experiment Telescope (EGRET) aboard the *Compton Gamma Ray Observatory* is sensitive to photons in the energy range from approximately 30 MeV to 30 GeV, using a multi-level spark chamber system to detect electron-positron pairs resulting from γ -rays. A NaI calorimeter provides energy resolution of 20-25%, and a plastic scintillator anti-coincidence dome prevents triggering on events not associated with high-energy photons. The detector thus has negligible background. The detector is described in more detail in Thompson et al. (1993) and references therein. The data sets used in this analysis consist of archival data, as well as PI data for Cycles 5 and 6. Data sets included event UTC arrival times accurate to 100 μ s, energy, measured direction of origin, satellite location, and other information. A summary of the observations of PSRs B1046–58 and J1105–6107 is presented in Tables 2 and 3.

2.1. Timing Analysis

The timing analysis was done using the interactive software `PULSAR` which has been described elsewhere (e.g. Fierro 1995) and is based on the `TEMPO` software package (e.g. Taylor & Weisberg 1989). Event arrival times are first reduced to the solar system barycenter and then folded using a contemporaneous ephemeris derived from radio monitoring.

Young pulsars are notorious for displaying timing irregularities, namely glitches and long-term timing “noise” (see Lyne 1996 for a review). The pulsars in question are no exception (Johnston et al. 1995, Kaspi et al. 1997). Timing noise alone can result in phase deviations as large as a full cycle over a year or two, while glitches can result in so large a phase deviation that only unusually dense observations can permit unambiguous phase determination. Such deviations cannot be tolerated when searching for γ -ray pulsations over many years, particularly when expecting weak pulsations, as even small deviations could broaden the signal beyond detectability.

For this reason, we have used contemporaneous radio ephemerides determined by timing observations made at the 64-m radio telescope at Parkes, Australia. Most radio observations were done at a central frequency near 1500 MHz, with some at 430 and 660 MHz. Prior to 1995, all data were obtained using filter-bank timing systems ($2 \times 64 \times 5$ MHz at 1520 MHz and $2 \times 256 \times 0.125$ MHz at 430 and 660 MHz) that have been described elsewhere (e.g. Bailes et al. 1994). Most data from after 1995 were obtained using the Caltech correlator-based pulsar timing machine (Navarro 1994), which has 2×128 lags across 128 MHz in each of two separate frequency bands. Typically, correlator observations were made at central frequencies of 1420 and 1650 MHz simultaneously. Filter-bank data were recorded on tape and folded off-line; correlator data were folded on-line. Resulting folded profiles were convolved with high signal-to-noise templates to yield topocentric pulse arrival times. Resulting arrival times were analyzed using the standard `TEMPO` pulsar timing software package⁶ together with the JPL DE200 ephemeris (Standish 1982). Ephemerides for folding the γ -ray data were determined piecewise using a minimum of some two dozen arrival times per valid interval, with RMS residuals well under the γ -ray binning resolution in all cases. The ephemerides used are provided for each EGRET viewing period in publicly accessible machine-readable format at <http://www.atnf.csiro.au/research/pulsar/psr/archive/>.

Since the range of radio frequencies observed at each epoch was not generally sufficiently large to determine dispersion measures with high precision, we assume that the dispersion measures do not vary significantly. Substantial variations would result in changes in the

⁶<http://pulsar.princeton.edu/tempo>

pulse phase extrapolated from the radio ephemeris to the effectively infinite γ -ray frequency according to the cold plasma dispersion law. This could cause smearing of the pulse profile. We can test the plausibility of our assumption of a constant dispersion measure (DM) using the results of Backer et al. (1993) who empirically characterized variations in DM for several pulsars. As neither pulsar considered here lies within a detectable supernova remnant (Johnston et al. 1995, Kaspi et al. 1996, Gotthelf & Kaspi 1998, Pivovarov, Kaspi, & Gotthelf 1999), the very large DM variations observed for the Crab and Vela pulsars, usually attributed to their unusual environments, are unlikely to be present. From the empirical findings of Backer et al. (1993), for PSR B1046–58, the maximum DM variation per year expected is $\sim 0.01 \text{ pc cm}^{-3}$. Over the ~ 8 yr duration of the experiment described here, this amounts to a variation in pulse phase of $\sim 1.2 \times 10^{-3}$, a factor of ~ 40 smaller than our binning resolution. For PSR J1105–6107, the DM variation could be an order of magnitude larger, however the experiment in this case spans only ~ 4 yr. The phase variation then could be as large as $\sim 1.1 \times 10^{-2}$, smaller, but only by a factor of ~ 4 , than our binning resolution. We conclude that DM variations are certainly negligible for PSR B1046–58, and probably negligible for PSR J1105–6107.

2.2. Spatial Analysis

The energy dependence of the point-spread function of the EGRET detector can be characterized by the function

$$\theta_{67}(E) = 5^\circ.85 \times (E/100)^{-0.534}, \quad (1)$$

where θ_{67} is the half-angle of the cone encircling the actual source direction and which contains 67% of the events having energy E in MeV (Thompson et al. 1993). In our timing analysis, we used all events within θ_{67} . The source directions are (J2000) RA $10^{\text{h}} 48^{\text{m}} 12^{\text{s}}.6(3)$, DEC $-58^\circ 32' 03''.75(1)$ for PSR B1046–58 (Stappers et al. 1999), and (J2000) RA $11^{\text{h}} 05^{\text{m}} 26^{\text{s}}.07(7)$, DEC $-61^\circ 07' 52''.1(4)$ for PSR J1105–6107 (Kaspi et al. 1997), where the numbers in brackets are 1σ uncertainties. The total number of counts folded is given for each viewing period in Tables 2 and 3 for PSRs B1046–58 and J1105–6107, respectively.

Spatial analysis of γ -ray data is done using the likelihood ratio test (Mattox et al. 1996). The significance of a point source is found using a test statistic T_s that compares the likelihood of the distribution of counts (which is governed by Poisson statistics) having occurred under the null hypothesis of no point source, with that with a point source present, given the instrumental point-spread function (PSF). Mattox et al. have shown that a point-

source significance in units of the standard deviation is given by $\sqrt{T_s}$ where

$$T_s \equiv 2(\ln L_1 - \ln L_0), \quad (2)$$

where L_1 is the likelihood under the assumption of a point source and L_0 is that under the null hypothesis. The likelihood itself is given by

$$L = \prod_{ij} \frac{\theta_{ij}^{n_{ij}} e^{-\theta_{ij}}}{n_{ij}!}, \quad (3)$$

where the product is over pixel ij that contains n_{ij} counts, and the model prediction is θ_{ij} .

3. Results

3.1. PSR B1046–58

3.1.1. Timing Analysis

In Figure 1, we present the folded light curve for PSR B1046–58 for energies above 400 MeV. The significance of the apparent modulation can only be established using appropriate statistical tests. The optimal test is the H-test (de Jager 1994), which provides a figure of merit for a folded light curve that is independent of the number of bins or of the phase of the putative signal. For this reason, the H-test is superior to the standard χ^2 test (e.g. Leahy et al. 1983). Further, the H statistic has been shown to be optimal when considering a light curve having unknown pulse morphology. In this sense, it is superior to the Z_N^2 test (Buccheri et al. 1983) which can be done for specified numbers of harmonics only. For the light curve in Figure 1, the H statistic is 22.5, which has a probability of 1.2×10^{-4} of having occurred by random chance, with 5 harmonics indicated. This corresponds to an equivalent normal distribution deviation of 3.9σ from the null hypothesis of no pulsations. For reference, $\chi^2 = 26.3$ for 10 bins (9 degrees of freedom); the probability of this value or higher having occurred by chance is 1.8×10^{-3} (3.1σ). The Z_4^2 statistic has value 33.8; the probability of this value or higher having occurred by chance is 4.3×10^{-5} (4.1σ). Note that there is effectively only a single trial folding period. Since we considered two pulsars, these probabilities should be multiplied by a factor of two. Although we did not search independent energy bands, the choice of 400 MeV lower energy cutoff was made to optimize the significance; we discuss this further below.

We have checked the robustness of our result in several ways. First, we divided the total data set into two halves of approximately equal size and verified that the signal is seen in

both, albeit at reduced significance, as expected. For the first half data set (MJDs 48386–49361), we find $H=16.7$, which has probability 1.3×10^{-3} , while for the second half data set (MJDs 49361–50728) we found $H=15.0$, having probability 2.4×10^{-3} . These statistics are for $E > 400$ MeV. Second, we verified that the signal persisted when the energy-dependent cone opening angle (Eq. 1) was increased to include 99% of the counts from the known source direction; in this case we found $H=12.5$, which has probability 6.8×10^{-3} .

Note that zero is suppressed in the light curve shown in Figure 1. The observed pulsed fraction for $E > 400$ MeV is 0.12 ± 0.02 . The off-pulse γ -rays may originate as diffuse Galactic emission — the pulsar is located in the complicated Eta Carina region, tangent to the Carina spiral arm, which is known to contain significant diffuse emission and many discrete sources. (Bertsch et al. 1993, Hunter et al. 1997). In §3.1.2 we describe a spatial analysis that indicates that a small fraction of the off-pulse could be emission from PSR B1046–58 itself.

One way to check for the presence of contaminating diffuse emission is to utilize the different expected spectra of diffuse and pulsed signals. In Figure 2 we show, in the lower panel, results of three statistical tests as a function of lower cutoff energy. The probability shown is that of finding the value of the statistical test, or higher, for a profile consisting of folded photons having energies above the cutoff. The upper panel shows the number of photons included in the analysis, here done for counts within θ_{67} . Qualitatively, the behavior is as expected: the diffuse emission has a softer spectrum than those of the known γ -ray pulsars, so as the lower energy bound is increased, the significance of the pulse should increase until the pulsar signal is too photon-starved to be detected. Furthermore, the EGRET PSF narrows with increasing energy (Eq. 1), so diffuse emission and nearby confusing point sources are preferentially removed as the lower energy bound is increased given advance knowledge of the pulsar position (Lamb & Macomb 1997). However, the sudden decrease in significance when the lower energy cut changes from 400 to 600 MeV is unexpected, given the smooth decrease in the number of counts. This could indicate a spectral cutoff in the pulsed emission, or could simply be a result of the poor statistics for the pulse profile; it could also suggest the apparently significant modulation is a statistical fluctuation.

The detection of pulsed high-energy γ -ray emission from PSR B1951+32 by Ramana-murthy et al. (1995) was done by considering events selected from a cone of fixed angle with respect to the pulsar position, as a compromise between maximizing signal from the source and minimizing background contamination. We have carried out the same analysis for PSR B1046–58, using a fixed cone of 2° half-angle. We chose this size cone as it resulted in a comparable total number of events as for the energy-dependent cone. For the fixed cone, we find $H= 23.9$, corresponding to a probability of 6.9×10^{-5} (4.0σ), an improvement over the energy-dependent-cone results. This supports the reality of the pulsations. However,

not all the profile statistics improve for the fixed cone; for example, the χ^2 statistic drops to 25.3, corresponding to a probability of 2.7×10^{-3} (3.0σ), still statistically significant, but less so than with the energy-dependent cone.

Ramanamurthy et al. (1996) reported high-energy γ -ray pulsations from the radio pulsar PSR B0656+14 using photons that had been “weighted” according to their energy and direction, and the known telescope response. We have employed a similar algorithm to theirs in considering the apparent modulation seen in the unweighted data. Each event is assigned a weight which is equal to the probability that a specific γ -ray originated from the point source (rather than as diffuse Galactic emission),

$$w = \frac{\text{PSF}(r, E)}{\text{PSF}(r, E) + \frac{B}{S}(E)}, \quad (4)$$

where $\text{PSF}(r, E)$ is the energy-dependent EGRET point spread function, the probability per steradian for a photon of energy E to be detected at a measured angle r from the source. B/S is the ratio of diffuse Galactic counts per steradian to source counts at energy E . As the combinations of weights within phase bins are, unlike the unweighted data, not described by Poisson statistics, the same statistical tests do not apply. Instead, we considered the simple statistical standard deviation of the binned values, x_i , $\sum_{i=1}^N (x_i - \bar{x})^2 / (N - 1)$. We used Monte Carlo simulations of profiles to determine the probability of chance occurrence of a profile having this statistic. Simulated profiles of weighted data were made by randomly varying the phases. In this way, for $E > 400$ MeV, we found that the probability of obtaining a profile having the same modified χ^2 statistic or higher for the folded, weighted data was 0.026. Thus the significance of the detection decreases using the weights. This was not expected. However, given the evidence below in favor of the association, it does not eliminate the possibility that pulsed flux is being detected from PSR B1046–58; the decrease in significance could be due to the poorly known pulsed γ -ray spectrum (which was assumed to be a power law of index 1.97 ± 0.07 – see §4.1.2) or to a statistical fluctuation.

3.1.2. Spatial Analysis

We have conducted a likelihood analysis (Mattox et al. 1996) of the EGRET data for PSR B1046–58 (see §2.2) for $E > 400$ MeV events. In the analysis, the model for the diffuse Galactic flux of Hunter et al. (1997) was used, and the flux of nearby sources in the Second EGRET catalog (Thompson et al. 1995) was estimated simultaneously with that from the position of PSR B1046–58. A point source at the pulsar position was detected with a significance of $\sqrt{T_s} = 10.8\sigma$. We estimate 347 ± 40 γ -ray events from this point source, corresponding to a flux of $(1.6 \pm 0.2) \times 10^{-7}$ photons $\text{cm}^{-2}\text{s}^{-1}$ ($E > 400$ MeV). The

distribution of EGRET events is consistent with the EGRET PSF; we find a reduced χ^2 of 1.3 for the sum of all events for Cycles 1–6 of the EGRET mission.

A similar analysis was done for different rotational phases. Phase-resolved event maps for $E > 400$ MeV were made for peak 1 (phases 0.300–0.475), interpeak 1 (0.475–0.675), peak 2 (0.675–0.825), and interpeak 2 (0.825–0.300). The peak 1 and peak 2 maps were combined to form an “on-pulse” map. The interpeak 1 and interpeak 2 maps were combined to form an “off-pulse” map.

For the on-pulse map, a point source at the position of PSR B1046–58 was detected with a significance of $\sqrt{T_s} = 10.2\sigma$, corresponding to an estimated 203 ± 25 γ -ray events. For the off-pulse map, a point source at the position of PSR B1046–58 was detected with a significance of $\sqrt{T_s} = 5.8\sigma$ corresponding to an estimated 144 ± 29 γ -ray events. The distribution of EGRET events was consistent with the PSF for both the on- and off-pulse phase selections. The EGRET position estimate was also consistent with that of PSR B1046–58 for both the on- and off-pulse phase selections. Thus, significant flux is detected during both the on- and off-pulse phases, and it appears that both the pulsar and diffuse Galactic γ -ray emission contribute to the emission represented by the suppressed zero in Figure 1.

We also subdivided the on-pulse map into two, by making separate maps for peak 1 and peak 2 data. Both peak 1 and peak 2 show a point source at the position of the pulsar, with significances of 6.0σ and 8.4σ , respectively.

Maps of “residual” flux were also made for both the on- and off-pulse phase selections by subtracting the counts distribution for nearby sources, counts corresponding to an isotropic flux of 0.295×10^{-5} photons $\text{cm}^{-2} \text{s}^{-1} \text{sr}^{-1}$, and counts corresponding to diffuse Galactic flux (with an empirically determined scaling factor of 0.242 for the model of Hunter et al. 1997 for $E > 100$ MeV flux). The residual counts map was then converted to a residual flux map by dividing by the exposure. The difference between the residual fluxes for the on- and off-pulse maps shows the expected distribution for the EGRET PSF with a source coincident with PSR B1046–58.

3.2. PSR J1105–6107

3.2.1. Timing Analysis

In Figure 3, we show the folded light curve for PSR J1105–6107 for energies above 400 MeV. The H statistic is 3.6, which has a probability of 0.24 of having occurred by chance. We thus find no evidence for γ -ray pulsations from PSR J1105–6107. We also tried folding

photons from within a cone encircling the source direction that contains 99% of the events; again no evidence for pulsations was found. We also searched for pulsations in different energy ranges to take advantage of the expected increased pulsed fraction with increasing low energy cutoff, but found no significant signals. Finally, we considered data weighted according to the algorithm described in §3.1, but again found no significant pulsations. The 99% confidence level upper limit on the pulsed fraction of 2EG J1103–6106 at the PSR J1105–6107 spin period for $E > 400$ MeV, using the H test and assuming a duty cycle of 0.5 is 0.33. For a duty cycle of 0.1, it is 0.13. For $E > 100$ MeV photons, the analogous limits are 0.09 and 0.04 for duty cycles 0.5 and 0.1, respectively.

4. Discussion

4.1. PSR B1046–58

The folded γ -ray profile for PSR B1046–58 and the spatial analysis of the γ -ray data provide evidence for the association between PSR B1046–58 and 2EG J1049–5847. However additional support for this conclusion is desirable, because of the difficulty in interpreting the pulse significance as a function of energy and the drop in significance when photon weighting is used. We consider here evidence that provides additional support for the association between PSR B1046–58 and 2EG J1049–5847.

4.1.1. ASCA X-Ray Observations of the 2EG J1049–5847 Field

Additional evidence in favor of associating PSR B1046–58 with 2EG J1049–5847 are the results of ASCA X-ray observations of the 2EG J1049–5847 field, which are described in a companion paper (Pivovarov, Kaspi, & Gotthelf 1999). There, archival ASCA observations are presented that cover the full 95% confidence error circle of the counterpart to 2EG J1049–5847 as determined by Hartman et al. (1999) in the recently published 3EG catalog (where the source name is 3EG J1048–5840). As Pivovarov et al. show, the only X-ray source within the 95% confidence contour of the γ -ray source is coincident with PSR B1046–58 within the $< 1'$ X-ray positional uncertainty. The source is unpulsed and is likely to be a synchrotron nebula. However, there is an additional nearby hard-spectrum X-ray source outside the 95% confidence contour (but within the 99% contour) that could also be the counterpart, a possibility we cannot rule out without an improved γ -ray source position. Nevertheless, the most likely counterpart from the X-ray observations is PSR B1046–58.

4.1.2. *Spectrum and Energetics*

Merck et al. (1996) found that 2EG J1049–5847 had a spectral index of 2.0 ± 0.1 , and noted that the γ -ray source had properties consistent with the known γ -ray pulsar population, as well as the positional coincidence with PSR B1046–58. Bertsch et al. (in preparation) find a spectral index of 1.97 ± 0.09 for the 3EG counterpart of 2EG J1049–5847, 3EG J1048–5840, and an integrated flux for $E > 100$ MeV of $(62 \pm 7) \times 10^{-8}$ photon $\text{cm}^{-2} \text{s}^{-1}$ (R. Hartman, personal communication). We have done an independent pulse-phase-resolved spectral analysis by considering the fluxes and spectra for peaks 1 and 2 separately, using γ -rays arriving during the off-peak 2 interval as a background estimate. We find spectra for both peaks that are consistent with that reported above as well as with each other.

Using the results of the on-pulse spatial analysis (§3.1.2) together with the reported 3EG point source flux (Hartman et al. 1999) and spectrum (Bertsch et al. 1999), we derive a pulsed flux for $E > 400$ MeV of $(2.5 \pm 0.6) \times 10^{-10}$ erg $\text{cm}^{-2} \text{s}^{-1}$, which corresponds to an efficiency for conversion of spin-down luminosity into pulsed $E > 400$ MeV γ -rays of 0.011 ± 0.03 for 1 sr beaming, assuming $d = 3$ kpc. Using the derived total pulsed fraction (§3.1.1), the total number of counts and the exposure yields consistent results. The observed flux is consistent with previously published upper limits (Thompson et al. 1994).

4.1.3. *Absence of Variability*

McLaughlin et al. (1996) quantified the variability of EGRET sources and showed that known γ -ray pulsars are not variable, in contrast to all known γ -ray-loud active galaxies for which accurate γ -ray flux measurements have been made. They further analyzed the variability of the unidentified EGRET sources and concluded that 2EG J1049–5847 is non-variable, consistent with its identification as an energetic rotation-powered pulsar. An analysis of the larger data set used to produce the 3EG catalog reveals no evidence for variability from the source, consistent with its identification as a rotation-powered pulsar (Hartman et al. 1999).

4.1.4. *Pulse Profile Morphology and Relative Radio Phase*

The morphology of the γ -ray profile shown in Figure 1 lends some support to its interpretation as pulsations from PSR B1046–58. Note that in the profile, the difference in height between the two peaks is not statistically significant, and the bin resolution is optimal. The two peaks, having separation 0.36 ± 0.13 in pulse phase, is reminiscent of the γ -ray profile of the Vela pulsar (e.g. Kanbach et al. 1994), which has comparable spin-down

parameters. Similar γ -ray pulse profiles are also observed for the Crab pulsar, Geminga, and PSR B1951+32 (Thompson 1996 and references therein). Hard X-ray observations of the Vela pulsar reveal a pulse profile that is similar to that at γ -ray energies (Strickman & Harding 1998); this suggests that hard X-ray observations of PSR B1046–58 could confirm its identification as a source of pulsed γ -rays. It must be kept in mind, however, that the profile of other well-established high-energy γ -ray pulsars is not as clearly double peaked. For example, PSR B1706–44, whose spin-down parameters most closely resemble those of PSR B1046–58, has a γ -ray profile whose morphology could be interpreted, within the limited statistics, as either single or double peaked with small peak separation. Therefore the double peaked profile in Figure 1 does not lend unambiguous support to the proposed association.

The γ -ray pulse’s offset from the single radio pulse (Fig. 1) is similar to those seen in the known high-energy γ -ray pulsars. The offset in time between the peak of the radio pulse and the approximate centroid of the first of the two γ -ray peaks shown in Figure 1 is 0.19 ± 0.12 in pulse phase, with the uncertainty dominated by the poor profile statistics. The phase offset to the approximate midpoint between the two apparent pulses is 0.37 ± 0.13 . The uncertainty in these numbers due to the uncertainty of 0.01 pc cm^{-3} in the single-epoch DM measurement (§1) is negligible. This offset is similar to those of the other γ -ray pulsars having similar γ -ray pulse morphologies, namely the Crab (considering the radio precursor as the analog of the PSR B1046–58 radio pulse), Vela, and PSR B1951+32 (Thompson 1996 and references therein). These show an approximate empirical trend of radio– γ -ray phase offset that increases with characteristic age (e.g. Thompson 1996). The observed radio/ γ -ray offset for PSR B1046–58 is in agreement with this trend, which predicts an offset in the approximate range 0.32–0.38.

4.1.5. Previous Discussion of the PSR B1046–58 / 2EG J1049–5847 Association

In addition to Thompson et al. (1994) noting a hint of a γ -ray pulsation from PSR B1046–58, Fierro (1995) discussed a possible association between the pulsar and 2EG J1049–5847 in detail. He noted the positional coincidence as well as the plausibility of the implied spectral and energy properties of the putative γ -ray pulsar. He also noted the absence of variability in the source. Yadigaroglu & Romani (1997) used a statistical test that quantifies the probability for positional coincidence of unidentified EGRET sources with nearby young objects. They identified the PSR B1046–58 / 2EG J1049–5847 association using this analysis. Zhang & Cheng (1998) argued that the PSR B1046–58 / 2EG J1049–5847 association was plausible on the basis of predictions from a version of the outer gap model of γ -ray

production in pulsar magnetospheres.

4.1.6. *Implications*

If the association between PSR B1046–58 and 2EG J1049–5847 is correct, then this is only the eighth pulsar to show evidence for high-energy γ -ray pulsations. The poor statistics in the folded profile and the presence of significant off-pulse emission preclude detailed analysis of the γ -ray emission properties. Nevertheless, the pulsar’s apparent γ -ray properties resemble those of other known γ -ray pulsars, particularly the Crab and Vela pulsars and PSR B1951+32 (radio and γ -ray pulse morphologies and phase offset). PSR B1046–58 further shares a property common to all other known “older” γ -ray pulsars (that is, excluding the Crab and PSR B1509–58), namely that its maximum luminosity appears to be in the high-energy γ -ray range. By contrast, Pivovarov et al. (1999) show that PSR B1046–58’s efficiency for conversion of \dot{E} into X-rays in the ASCA range is only $\sim 1 \times 10^{-4}$.

We now consider what the implications of the possible γ -ray pulsations from PSR B1046–58 are for models of γ -ray emission from rotation-powered pulsars. If the pulsations are real, the observed phase offset of the radio pulse is difficult to understand in the context of models in which the γ -rays are produced by particles which are accelerated along open field lines near the neutron star by electric fields (e.g. Dougherty & Harding 1982, Dermer & Sturmer 1994). In these models, the radio emission is thought to arise in the same polar cap region, so the radio pulse should be observed between the γ -ray peaks, which result from emission from a hollow cone. The conal geometry results from the smaller radius of curvature of magnetic field lines near the polar cap rim (see Harding 1996 for a review). This radio/ γ -ray phase problem has been noted for other γ -ray pulsars as well, e.g. Vela (Daugherty & Harding 1996); the results reported here argue that the problem is general. Also, emission beams in the polar cap model tend to be narrow and aligned with the magnetic and spin axes (e.g. Sturmer & Dermer 1994, Harding & Muslimov 1998); this can pose a problem for the pulsar birth rate. However, the radio phase offset problem, as argued by Harding & Muslimov (1998), seems general to both the polar cap γ -ray emission model as well as to geometric models of thermal X-ray pulsations, while the relative phases of the latter two are consistent. Polar cap models therefore make a testable prediction regarding the phase of the peak of any thermal X-ray emission that may one day be detected from PSR B1046–58.

The observed γ -ray pulse morphology and radio phase offset for PSR B1046–58 are, by contrast, well explained in the outer gap model. In this model, the γ -ray emission is produced in the charge-depleted region between the closed magnetic field lines and the velocity of light cylinder (e.g. Cheng, Ho, & Ruderman 1986, Chiang & Romani 1994, Romani & Yadigaroglu

1995, Zhang & Cheng 1998). The double peaked γ -ray pulse morphology in this model arises from a single pole's outer gap that has uniform emissivity along its field lines but in which the radiation is subject to significant relativistic aberration and time-of-flight delays through the magnetosphere; the expected pulse morphology for most viewing geometries is double peaked, as long as the magnetic inclination is not small. The morphology and phase are also consistent with the geometry proposed by Manchester (1996) in which the radio emission is produced in the outer gap as well. The outer gap model predicts bridge emission between the two γ -ray peaks, whose outer edges should be sharp; this could be tested with an improved γ -ray pulse profile. This model results in large beaming fractions that are consistent with the pulsar birth rate; this implies that most, if not all, of the unidentified EGRET low-latitude sources that have constant fluxes are young rotation-powered pulsars (Yadigaroglu & Romani 1997), although most of them will not be detectable in radio waves from Earth because of smaller radio beaming fractions. We note, however, that recently reported very tentative evidence for γ -ray emission from the millisecond pulsar PSR J0218+4232 (Kuiper et al. 1998) could pose a problem for the outer gap model, which predicts that millisecond pulsars should not be detectable in high-energy γ -rays (Romani & Yadigaroglu 1995).

4.1.7. *Unpulsed γ -ray Emission from PSR B1046–58?*

The spatial analysis of the EGRET data presented in §3.1.2 showed evidence for off-pulse emission consistent with coming from a point source coincident with the pulsar. For $E > 400$ MeV, this emission has flux $(1.9 \pm 0.6) \times 10^{-10}$ erg cm $^{-2}$ s $^{-1}$, which corresponds to $\sim 10\%$ of \dot{E} , for isotropic emission. The poor spatial resolution of EGRET obviously precludes a firm association between the pulsar and this unpulsed emission, although we note that off-pulse γ -ray emission has been seen for the Crab, Vela and Geminga pulsars, with that of the Crab possibly originating in the surrounding nebula (Fierro et al. 1998).

4.2. PSR J1105–6107

Since we find no evidence for γ -ray pulsations for PSR J1105–6107, we set an upper limit on the fraction of \dot{E} that is converted into high-energy γ -rays beaming in our direction. The counterpart to 2EG J1103–6106 in the 3EG catalog, 3EG J1102–6103, has flux $(32.5 \pm 6.2) \times 10^{-8}$ photons cm $^{-2}$ s $^{-1}$ for $E > 100$ MeV, and photon index 2.47 ± 0.21 (Hartman et al. 1999). Using these numbers, we infer with 99% confidence that PSR J1105–6107 converts less than 8×10^{-11} erg cm $^{-2}$ s $^{-1}$ and 3×10^{-11} erg cm $^{-2}$ s $^{-1}$ for duty cycles of 0.5 and 0.1, respectively. These limits correspond to efficiencies for conversion of spin-down luminosity of

less than 0.014 and 0.006 for 1 sr beaming and assuming a distance of 7 kpc, for duty cycles 0.5 and 0.1, respectively. These limits are not constraining on models of γ -ray emission.

5. Conclusions

We have found evidence for γ -ray emission from the young, energetic radio pulsar PSR B1046–58, which, if correct, establishes a counterpart for the previously unidentified high-energy γ -ray source 2EG J1049–5847 (GEV J1046–5840, 3EG J1048–5840). The evidence can be summarized as follows. (i) PSR B1046–58 has the ninth highest value of \dot{E}/d^2 of the known radio pulsars, with six of the eight higher slots occupied by known γ -ray pulsars. This suggests that PSR B1046–58 is likely to be detectable in γ -rays. (ii) The radio pulsar is spatially coincident with the unidentified EGRET source 2EG J1049–5847. (iii) The folded light curve for $E > 400$ MeV, obtained using contemporaneous radio ephemerides, is characterized by an H-test statistic 22.5; the chance probability of this value or higher having occurred is 1.2×10^{-4} . This number should be multiplied by a factor of two for the two pulsars we searched. (iv) A spatial likelihood analysis of on- and off-pulse data reveals a point source coincident with the radio pulsar position whose significance is much greater on-pulse than off (10.2σ versus 5.8σ). (v) The only hard X-ray point source detected in the 95% EGRET error box is spatially coincident with the pulsar (Pivovarov et al. 1999). (vi) The γ -ray light curve morphology resembles those of other the known γ -ray pulsars (the Crab and Vela pulsars, Geminga, and PSR B1951+32), namely, two narrow peaks separated by ~ 0.4 in pulse phase. (vii) The inferred radio/ γ -ray phase offset is consistent with trends seen for other pulsars. The implied efficiency for conversion of spin-down energy into $E > 400$ MeV γ -rays, 0.011 ± 0.003 for $d = 3$ kpc and 1 sr beaming, is consistent with those seen for other pulsars. We also found evidence for spatially unresolved unpulsed γ -ray emission from the pulsar position, as has been reported for the Crab, Vela and Geminga pulsars.

If the association between PSR B1046–58 and 2EG J1049–5847 emission exists, it should be confirmed by GLAST, the planned Gamma-ray Large Area Space Telescope, which will provide significantly higher angular resolution and more detector area than EGRET. It may be possible to confirm the γ -ray pulsations by detecting magnetospheric X-ray pulsations from PSR B1046–58 at hard X-ray energies. The similarity of this pulsar’s rotational parameters and high-energy γ -ray efficiency to those of PSR B1706–44 suggest TeV emission might be detectable. Thermal emission from the initial cooling of this young neutron star may also be detectable.

If the association between PSR B1046–58 and 2EG J1049–5847 holds, that seven of the top nine pulsars ranked by \dot{E}/d^2 are γ -ray pulsars (with one of the two remainders not

having been studied at γ -ray energies – see Table 1) implies at the very least that the radio and γ -ray beams are aligned closely, or that γ -ray beams are wide. In fact, the morphology of the observed γ -ray pulse and the phase offset of the radio pulse provide support for the outer gap model of γ -ray emission (Romani & Yadigaroglu 1995 and references therein). This model predicts that an improved γ -ray profile should find bridge emission between the pulses whose outer edges should be sharp. In this model, most or all of the unidentified EGRET sources that have constant fluxes are young rotation-powered pulsars like PSR B1046–58, though most radio beams will not be detectable from Earth due to small radio beaming fractions.

Our analysis of EGRET data from the direction of PSR J1105–6107 finds no evidence for γ -ray pulsations. This pulsar converts at most 0.014 (99% confidence) of its spin-down power to $E > 100$ MeV γ -rays beamed in our direction, assuming 1 sr beaming, a duty cycle of 0.5, and a distance to the source of 7 kpc. This limit is not constraining on models.

Acknowledgements

We are grateful to Dave Thompson for many helpful conversations, and Robert Hartman for communication of Third EGRET Catalog numbers prior to publication. We also thank Russell Pace for help with the Parkes observations. This research has made use of data obtained through the High Energy Astrophysics Science Archive Research Center Online Service, provided by the NASA/Goddard Space Flight Center. This work was supported by NASA grants NAG 5-3178 and NAG 5-3683 to VMK, and NASA LTSA grant NAG 5-3384 to JRM. We thank Joe Fierro for inspiration and assistance in the initial undertaking of this project.

REFERENCES

- Backer, D. C., Hama, S., Van Hook, S., & Foster, R. S. 1993, *ApJ*, 404, 636
- Bailes, M. et al. 1994, *ApJ*, 425, L41
- Bertsch, D. L., Dame, T. M., Fichtel, C. E., Hunter, S. D., Sreekumar, P., Stacy, J. G., & Thaddeus, P. 1993, *ApJ*, 416, 587
- Buccheri, R. et al. 1983, *A&A*, 128, 245
- Caraveo, P. A., Bignami, G. F., Mignani, R., & Taff, L. G. 1996, *ApJ*, 461, 91
- Cheng, K. S., Ho, C., & Ruderman, M. 1986, *ApJ*, 300, 500
- Cheng, K. S. & Zhang, L. 1998, *ApJ*, 498, 327
- Chiang, J. & Romani, R. W. 1994, *ApJ*, 436, 754
- Crawford, F., Kaspi, V. M., Manchester, R. N., & Lyne, A. G. 1999, in preparation
- Daugherty, J. K. & Harding, A. K. 1996, *ApJ*, 458, 278
- de Jager, O. C. 1994, *ApJ*, 436, 239
- Dermer, C. D. & Sturmer, S. J. 1994, *ApJ*, 420, L75
- Dougherty, J. K. & Harding, A. K. 1982, *ApJ*, 252, 337
- Esposito, J. A., Hunter, S. D., Kanbach, G., & Sreekumar, P. 1996, *ApJ*, 461, 820
- Fierro, J. M. 1995. PhD thesis, Stanford University
- Fierro, j. M., Michelson, P. F., Nolan, P. L., & Thompson, D. J. 1998, *ApJ*, 494, 734
- Gotthelf, E. V. & Kaspi, V. M. 1998, *ApJ*, 497, L29
- Harding, A. K. 1996, in *Pulsars: Problems and Progress*, IAU Colloquium 160, eds. S. Johnston, M. A. Walker, & M. Bailes, San Francisco, Astronomical Society of the Pacific, 315
- Harding, A. K. & Muslimov, A. G. 1998, *ApJ*, 500, 862
- Hartman, R. C. et al. 1999, *ApJ*. in press
- Hunter, S. D. et al. 1997, *ApJ*, 481, 205

- Johnston, S., Lyne, A. G., Manchester, R. N., Kniffen, D. A., D’Amico, N., Lim, J., & Ashworth, M. 1992, MNRAS, 255, 401
- Johnston, S., Manchester, R. N., Lyne, A. G., Kaspi, V. M., & D’Amico, N. 1995, A&A, 293, 795
- Kaaret, P. & Cottam, J. 1996, ApJ, 462, L35
- Kanbach, G. et al. 1994, A&A, 289, 855
- Kanbach, G. et al. 1996, A&AS, 120, 461
- Kaspi, V. M., Bailes, M., Manchester, R. N., Stappers, B. W., & Bell, J. F. 1996, Nature, 381, 584
- Kaspi, V. M., Bailes, M., Manchester, R. N., Stappers, B. W., Sandhu, J. S., Navarro, J., & D’Amico, N. 1997, ApJ, 485, 820
- Kaspi, V. M., Crawford, F., Manchester, R. N., Lyne, A. G., Camilo, F., D’Amico, N., & Gaensler, B. M. 1998, ApJ, 503, L161
- Kuiper, L., Hermsen, W., Verbunt, F., Belloni, T., & Lyne, A. 1998, in Proceedings of the 3rd INTEGRAL Workshop: The Extreme Universe, <http://xxx.lanl.gov/abs/astro-ph/9812408>
- Lamb, R. C. & Macomb, D. J. 1997, ApJ, 488, 872
- Leahy, D. A., Darbro, W., Elsner, R. F., Weisskopf, M. C., Sutherland, P. G., Kahn, S., & Grindlay, J. E. 1983, ApJ, 266, 160
- Lyne, A. G. 1996, in Pulsars: Problems and Progress, IAU Colloquium 160, eds. S. Johnston, M. A. Walker, & M. Bailes, San Francisco, Astronomical Society of the Pacific, 73
- Manchester, R. N. 1996, in Pulsars: Problems and Progress, IAU Colloquium 160, eds. S. Johnston, M. A. Walker, & M. Bailes, San Francisco, Astronomical Society of the Pacific, 193
- Marshall, F. E., Gotthelf, E. V., Zhang, W., Middleditch, J., & Wang, Q. D. 1998, ApJ, 499, L179
- Mattox, J. R. et al. 1996, ApJ, 461, 396
- McLaughlin, M. A., Mattox, J. R., Cordes, J. M., & Thompson, D. J. 1996, ApJ, 473, 763

- Merck, M. et al. 1996, *A&AS*, 120, 465
- Navarro, J. 1994. PhD thesis, California Institute of Technology
- Pivovarov, M., Kaspi, V. M., & Gotthelf, E. V. 1999, *ApJ*, submitted
- Qiao, G. J., Manchester, R. N., Lyne, A. G., & Gould, D. M. 1995, *MNRAS*, 274, 572
- Ramanamurthy, P. V. et al. 1995, *ApJ*, 447, L109
- Ramanamurthy, P. V., Fichtel, C. E., Kniffen, D. A., Sreekumar, P., & Thompson, D. J. 1996, *ApJ*, 458, 755
- Romani, R. W. & Yadigaroglu, I.-A. 1995, *ApJ*, 438, 314
- Standish, E. M. 1982, *A&A*, 114, 297
- Stappers, B. W., Gaensler, B. M., Johnston, S., & Frail, D. A. 1999. in preparation
- Steinberger, J., Kaspi, V. M., & Gotthelf, E. V. 1999, in *Proceedings of the Elba Workshop: Neutron Stars and Supernova Remnants*, *Memorie della Societa' Astronomica Italiana*, in press
- Strickman, M. S. & Harding, A. K. 1998, *BAAS*, 192, 74.04
- Sturmer, S. J. & Dermer, C. D. 1994, *ApJ*, 420, L79
- Sturmer, S. J. & Dermer, C. D. 1995, *A&A*, 293, L17
- Swanenburg, B. N. et al. 1981, *ApJ*, 243, L69
- Taylor, J. H. & Cordes, J. M. 1993, *ApJ*, 411, 674
- Taylor, J. H. & Weisberg, J. M. 1989, *ApJ*, 345, 434
- Thompson, D. J. et al. 1993, *ApJS*, 86, 629
- Thompson, D. J. et al. 1994, *ApJ*, 436, 229
- Thompson, D. J. et al. 1995, *ApJS*, 101, 259
- Thompson, D. J. 1996, in *Pulsars: Problems and Progress*, IAU Colloquium 160, eds. S. Johnston, M. A. Walker, & M. Bailes, San Francisco, Astronomical Society of the Pacific, 307
- Thompson, D. J. et al. 1999, *ApJ*, in press

Torii, K. et al. 1998, ApJ, 494, L207

Ulmer, M. P. et al. 1993, ApJ, 417, 738

Yadigaroglu, I.-A. & Romani, R. W. 1995, ApJ, 449, 211

Yadigaroglu, I. A. & Romani, R. W. 1997, ApJ, 476, 347

Zhang, L. & Cheng, K. S. 1998, A&A, 335, 234

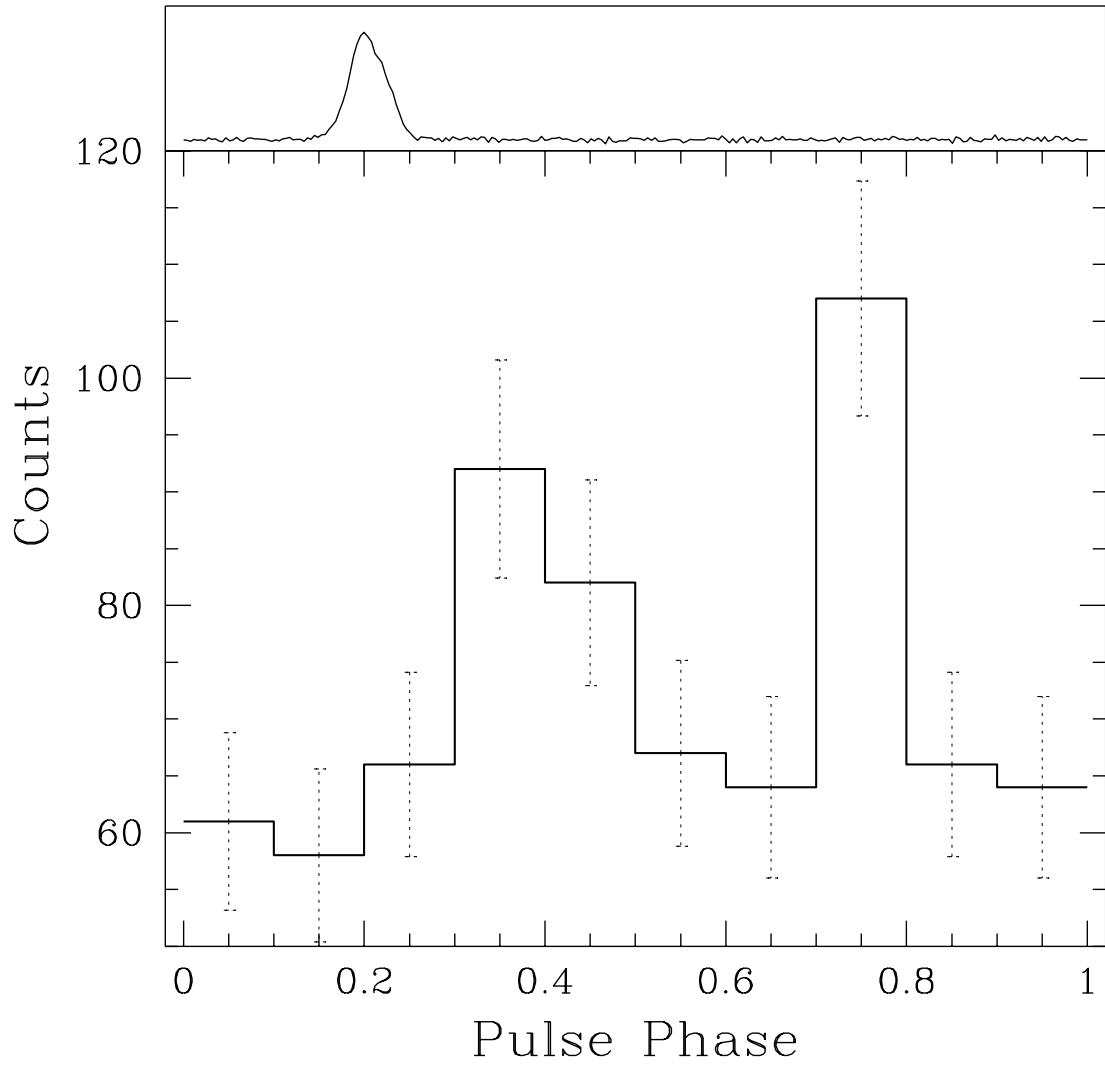


Fig. 1.— Bottom panel: folded EGRET light curve for PSR B1046–58 for $E > 400$ MeV. Top panel: radio profile at 20 cm from the Parkes observatory.

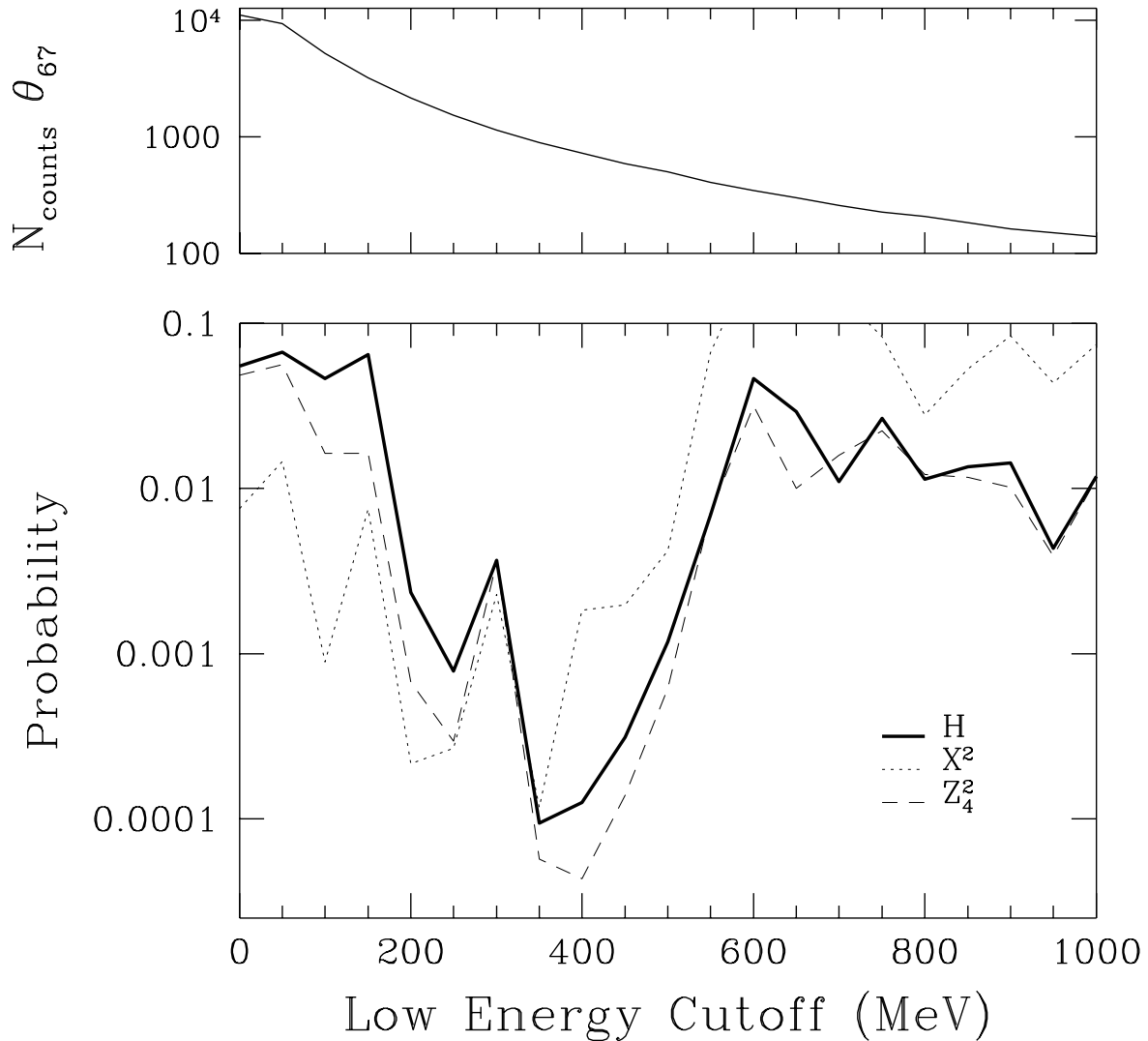


Fig. 2.— Upper panel: number of events within θ_{67} for PSR B1046–58 as a function of lower energy cutoff in MeV. Lower panel: results of three statistical tests applied to folded profiles for PSR B1046–58 as a function of lower energy cutoff in MeV. The probabilities represent the chance of the measured value of the statistical test or higher having been obtained by chance. The three tests are the H test, the χ^2 test for 10 bins (9 degrees of freedom), and the Z_4^2 test.

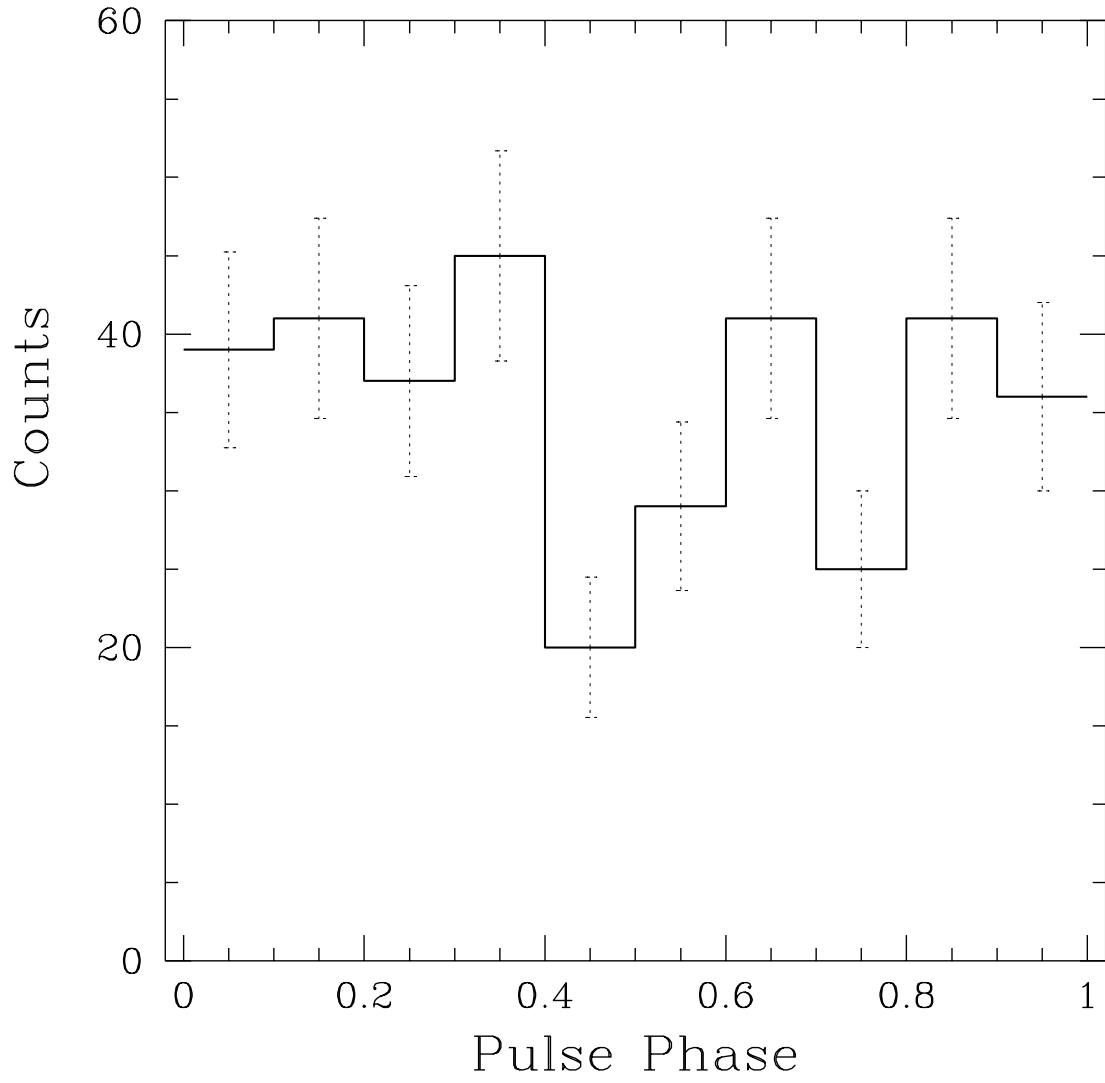


Fig. 3.— Folded EGRET light curve for PSR J1105–6107 for $E > 400$ MeV.

Table 1. Summary of Known High-Energy γ -ray Pulsars and PSRs B1046–58 and J1105–6107, ordered by τ .

Pulsar ^a	P ms	$\log \tau^b$ yr	$\log B^c$ G	$\log \dot{E}^d$ erg s ⁻¹ cm ⁻²	d^e kpc	\dot{E}/d^2 ^f rank	η_γ^g %
Crab	33	3.1	12.6	38.7	2.0	1	0.013±0.006
Vela	89	4.1	12.5	36.8	0.5	2	0.18±0.07
B1706–44	102	4.2	12.5	36.5	1.8	4	0.72±0.47
B1046–58	124	4.3	12.5	36.3	3.0	9	1.1±0.3
J1105–6107	63	4.8	12.0	36.4	7.1	23	< 1.4
B1951+32	39	5.0	11.7	36.6	2.4	6	0.26±0.17
B0656+14	385	5.0	12.7	34.6	0.8	20	~0.1
Geminga	237	5.5	12.2	34.5	0.157 ^{+0.059} _{-0.034}	3	1.61 ^{+0.22} _{-0.08}
B1055–52	197	5.7	12.0	34.5	1.5	39	6–13

^aPulsars in bold are the subject of this paper.

$$^b\tau \equiv P/2\dot{P}$$

$$^cB \equiv 3.2 \times 10^{19}(P\dot{P})^{1/2} \text{ G}$$

$$^d\dot{E} \equiv 4\pi^2 I \dot{P}/P^3$$

^eDistances from Taylor & Cordes (1993) except for Geminga which is from Caraveo et al. (1996).

^fRanked 5th is PSR B1509–58, detected in low-energy γ -rays (Ulmer et al. 1993); 7th is the millisecond pulsar PSR J0437–4715; 8th is PSR J1617–5055, which was only recently discovered (Torii et al. 1998, Kaspi et al. 1998).

^gFor $E > 100$ MeV and 1 sr beaming, except for PSR B1046–58 which is for $E > 400$ MeV. Uncertainties include nominal distance uncertainties. Numbers are from Fierro (1995) except for Geminga, for which we have used the updated distance, PSR B0656+14, which is from Ramanamurthy et al. (1996), and PSR B1055–52, which is from Thompson et al. (1999). For PSR J1105–6107, the 3σ upper limit for duty cycle 0.5 is quoted.

Table 2. Summary of EGRET Observations for PSR B1046–58.

VP ^a	MJD Range	$\Delta\theta^b$ ◦	$N(\theta_{67})$	Exposure
0007	48386–48392	21.1	614	0.52
0060	48463–48476	31.2	279	0.54
0080	48490–48504	25.2	1032	1.01
0120	48546–48560	31.3	235	0.49
0140	48574–48588	2.7	3252	3.08
0170	48617–48631	32.4	140	0.45
0230	48700–48714	34.8	30	0.14
0320	48798–48805	22.5	289	0.40
2080	49020–49027	28.1	163	0.18
2150	49078–49083	32.4	52	0.08
2170	49089–49097	32.4	34	0.12
2300	49195–49198	11.1	335	0.45
2305	49198–49202	8.7	416	0.60
3010	49216–49223	24.1	361	0.40
3140	49355–49368	16.8	775	1.09
3150	49368–49375	16.8	381	0.60
3160	49375–49384	28.7	157	0.24
3385	49595–49615	24.1	649	0.87
4020	49643–49650	23.5	156	0.24
4025	49650–49657	19.8	195	0.40
4150	49818–49832	27.1	261	0.36
4240	49908–49923	30.9	65	0.24
5220	50245–50248	2.7	136	0.33
5310	50359–50371	3.7	366	1.16
6270	50693–50700	1.6	234	1.01
6300	50714–50728	1.6	437	1.89

^aEGRET Viewing Period.

^bAngular offset of pulsar from center of EGRET field of view.

Table 3. Summary of EGRET Observations of PSR J1105–6107.

VP ^a	MJD Range	$\Delta\theta^b$ °	$N(\theta_{67})$	Exposure
2300	49195–49198	14.0	293	0.38
2305	49198–49202	11.8	412	0.52
3010	49216–49223	27.0	245	0.30
3140	49355–49368	13.7	826	1.32
3150	49368–49375	13.7	420	0.71
3160	49375–49384	26.9	213	0.27
3385	49595–49615	27.0	430	0.67
4020	49643–49650	20.4	201	0.32
4025	49650–49657	16.7	226	0.31
4150	49818–49832	28.0	213	0.35
4240	49908–49923	28.9	114	0.28
5220	50245–50248	5.0	128	0.32
5310	50359–50371	6.7	304	0.99
6270	50693–50700	3.6	205	0.96
6300	50714–50728	3.6	419	1.81

^aEGRET Viewing Period.

^bAngular offset of pulsar from center of EGRET field of view.